



## Sludge dewatering and drying: about the difficulty of making experiments with a non-stabilized material

Y.B. Pambou\*, L. Fraikin, T. Salmon, M. Crine, A. Léonard

*Laboratory of Chemical Engineering, Department of Applied Chemistry, University of Liège, B6c Sart Tilman, 4000 Liège, Belgium, Tel. +3243663515; Fax: +3243662818; email: yvon-bert.pambou@student.ulg.ac.be (Y.B. Pambou), Tel. +3243663519; Fax: +3243662818; emails: laurent.fraikin@ulg.ac.be (L. Fraikin), t.salmon@ulg.ac.be (T. Salmon), Tel. +3243663559; Fax: +3243662818; email: m.crine@ulg.ac.be (M. Crine), Tel. +324366354436; Fax: +3243662818; email: a.leonard@ulg.ac.be (A. Léonard)*

Received 20 February 2014; Accepted 5 June 2015

---

### ABSTRACT

Due to increasing amounts of wastewater bio-sludges produced worldwide, a lot of research has been carried out to optimize their treatment in view of reducing their high water content. Large efforts have been made on bio-sludge conditioning prior to mechanical dewatering. Research about drying is more recent but becomes more and more important in order to produce pellets that can safely be used in agriculture or that can be incinerated to recover energy. The consequences of the dewatering step especially, the nature and dosage of the polymer used for conditioning, on further drying still need to be investigated. However, such studies require making a large number of experiments at the laboratory scale, which needs to use a liquid bio-sludge with constant properties in order to get relevant results. Within this context, this article emphasizes the difficulty of making experiments with an organic material, by showing dewatering and drying results obtained during two series of tests. The experiments were conducted with bio-sludge collected after thickening in a local wastewater treatment plant. During the first test series “W,” experiments, i.e. conditioning, dewatering and drying, were performed on three samples with one week apart, using the same initial bio-sludge. For the second series “D,” trials were done each day during a working week. The Zetag 7587 conditioner was used to evaluate bio-sludge flocculation behaviors. The dewatering was made using a normalized filtration-expression cell. Drying experiments were carried out in a convective micro-dryer. The results indicate that an increase in storage duration leads to changes in bio-sludge dewatering and drying behaviors, leading to poor repeatability of experiments. Consequently, any experimental design must be completed in a limited time span to obtain relevant results. About shrinkage response which develops during drying, a two-zone linear model was developed. It was observed that the first part of the curve was almost similar for all experiments, whereas the second part reached progressively to lower volumes with increasing storage duration. In future works, the impact of other polyelectrolytes’ type and dosage at the laboratory scale on the dewatering and drying processes will be investigated more deeply.

*Keywords:* Wastewater bio-sludge treatment; Bio-sludge flocculation; Dewatering; Convective drying; X-ray microtomography

---

\*Corresponding author.

## 1. Introduction

According to the directive of the Council of European Communities concerning urban wastewater treatment [1], municipalities will have to face with growing amounts of wastewater bio-sludge, because of the multiplication of the number of wastewater treatment plants. This production is expected to double in the European Union during the next 10 years [2]. At the same time, the directive on waste landfill [3] has planned the progressive reduction of bio-sludge disposal in dump sites until 2016 [4,5]. At the present time, two major issues are used for bio-sludge disposal: energy valorization through incineration and agriculture valorization through landspreading [5].

Excess bio-sludge which is produced by the biological treatment of wastewater still contains more than 99% of water at the bottom of thickeners. A further mechanical dewatering step is essential prior to drying. However, bio-sludge is a colloidal system in which small bio-sludge particles form a stable suspension in water, making them very difficult to be separated from the water phase. The poor bio-sludge dewaterability is in great extent related to the presence of extracellular polymeric substances (EPS) which induce a negative surface charge of the bio-sludge flocs [6], bio-sludge solids composition [7] and its rheological properties. This complex process can also be influenced by external factors such as the choice of the dewatering equipment type and driving force (gravity, pressure and vacuum) [8].

To enhance bio-sludge dewaterability, the addition of chemical conditioners such as flocculants and/or coagulants is often necessary to help the bio-sludge particles to agglomerate into larger settleable flocs prior to solid–water separation, usually by mechanical dewatering device. Depending on the dewatering technique, the so-called bio-sludge cake reaches around 15–35% of dry solids content (DS), which represents the total solids captured after water removal. Thermal drying can then be used to remove totally or partially the remaining water, depending on bio-sludge final use. This obviously reduces the mass and volume of waste and, consequently, the cost for storage, handling, and transport. The removal of water to such a low level also increases drastically the lower calorific value, transforming the bio-sludge into an acceptable combustible [9].

Even though the conditioning and dewatering steps are known to have an impact on bio-sludge drying behavior, practically no study can be found about the role of the flocculants' nature and dosage. Before studying experimentally the influence of polymer's type and dosage on dewatering performances and

subsequent drying behavior, it is necessary to assess the bio-sludge variability with storage duration because bio-sludge is a highly fermentable material whose properties and composition can rapidly change. Few studies have been performed on the impact of the storage duration of non-conditioned liquid bio-sludge. Raynaud et al. [10] showed that good repeatability could be obtained for three successive days when liquid bio-sludge, beforehand concentrated and diluted to the desired concentration, was stored at 4°C. Some groups focused on the stability of dewatered bio-sludge samples directly collected in a wastewater treatment plant, with regard to their drying behavior or associated gaseous emissions. Fraikin et al. [11] clearly showed the impact of both the storage duration and the temperature on bio-sludge convective drying properties. Ferrasse et al. [12] focused on indirect agitated drying. They showed that experiments remained repeatable up to 8 or 9 d, but disregarded the results of the first two days.

Within this context, the aim of the present work is to illustrate the impact of non-conditioned liquid bio-sludge storage duration on its dewatering and drying behavior, prior to the realization of larger experimental campaigns. The method to be used consists in determining the adequate polymer dosage in the flocculation step and then repeating dewatering and drying tests with this same polymer concentration on the same wastewater bio-sludge after different periods of bio-sludge storage. Although most of the research (not all) at the laboratory scale showed that bio-sludge samples have to be stored at 4°C prior to starting the dewatering tests, this procedure can be questionable because the bio-sludge storage temperature maybe selected according to industrial purposes. For example, Bruus et al. [13] have studied the effects of anaerobic bio-sludge storage prior to dewatering. These authors stored their bio-sludge samples at room temperature before starting any experimental tests. For this reason, it can be argued that 4°C is not the only temperature that has to be taken into account with implication to improving the dewatering and drying process. In this work, it was decided to keep the bio-sludge samples at room temperature in order to stay as close as possible to industrial reality.

In fact, at the industrial scale, there are several possibilities concerning bio-sludge storage. Within large WWTPs, the bio-sludge is collected at the bottom of thickeners. The dewatering process is performed just after the conditioning of the thickened bio-sludge. In that case, no real storage is done but a rather continuous treatment can be done with bio-sludge properties remaining quite stable. Conversely, in some

small-/medium-size WWTPs, a continuous treatment would not be economically relevant. In that case, the thickened bio-sludge is stored in an aerated tank for several production days (up to 4). Then the whole batch is conditioned and dewatered.

## 2. Materials and methods

### 2.1. Bio-sludge samples

The study was performed on activated bio-sludge samples collected after thickening from the wastewater treatment plant of the Grosses-Battes, located close to the University of Liège (Belgium). This plant is designed for treatment of domestic wastewater from a part of the city of Liège in an amount of 59,041 PE (population equivalent). Operating on the principle of activated bio-sludge, the plant has removal of total organic carbon, nitrogen as well as phosphorous by biological process. After transportation to the laboratory, the bio-sludge samples were stored at room temperature of  $25 \pm 2^\circ\text{C}$  in open vessels under continuous gentle stirring. At this temperature, the industrial purpose can be well simulated.

### 2.2. Evaluation of raw bio-sludge characteristics (Standard Methods)

Before bio-sludge was used in the flocculation step, its characteristics in terms of dry solids (DS) and volatile solids (VS) content were determined at the beginning of each experiment, according to standard methods [14]. Precisely, the DS and VS content of raw bio-sludge were, respectively, determined by drying repetitively the wet material at  $105^\circ\text{C}$  until mass stabilization (usually 24 h), then by calcinating the dried residue at  $550^\circ\text{C}$  for 2 h, and weighing. Three replicated tests were carried out to evaluate the reliability of the experiments. Finally, the DS and VS content of raw bio-sludge as percent (%) were estimated according to, respectively, (Eqs. (1) and (2)).

$$\text{DS} = \frac{W_d - W_p}{W_s - W_p} \times 100 \quad (1)$$

where DS is the total solids content of the control sample (%);  $W_d$  is the total weight of the control including the weighting dish (g), after drying at  $105^\circ\text{C}$ ;  $W_p$  is the tare weight of the weighting dish (g);  $W_s$  is the weight of control, before drying (g).

$$\text{VS} = \left(1 - \frac{W_q - W_r}{W_t - W_r}\right) \times 100 \quad (2)$$

where VS is the volatile solids content of the sample (%);  $W_q$  is the total weight of the dried sample including the weighting dish (g), after calcination at  $550^\circ\text{C}$ ;  $W_r$  is the tare weight of the weighting dish (g);  $W_t$  is the total weight of the dried residue obtained at  $105^\circ\text{C}$  including the weighting dish (g).

### 2.3. Bio-sludge conditioning

Zetag 7587 provided in powder form (Ciba, Belgium) was used to evaluate bio-sludge flocculation behavior. This polymer was chosen for its large use in wastewater treatments. A diluted polymer solution (1 g/L) was prepared the day before its use. A classical Jar test device (Floctest, Bioblock Scientific 82993) was used to mix the polymer with the bio-sludge. Samples of 600 mL of bio-sludge were put in a beaker of 800 mL. The polymer was added rapidly in the stirred vessel while the bio-sludge was quite intensely stirred (120 rpm for 1 min) to promote polymer dispersion. After this period, the rotation speed was reduced and the bio-sludge was gently stirred at 40 rpm for 3 min to promote floc growth.

For easiness and quickness, the Jar test method was used to determine good dosage requirements for chemical-added polymer. The setup consists in six axial mixing bladed paddles that are operated by a single motor, so mixing conditions are the same in the six beakers, and each one was filled with 600 mL of the raw bio-sludge sample. A range from 2 to 12 g/kg<sub>DS</sub> of polymer doses was tested. Visual observations were used to evaluate the effectiveness of the dosage such as more stable and larger floc particles, faster settling and better clarity of the supernatant. Using this method, the best polymer dosage was found close to 8 g/kg<sub>DS</sub>.

### 2.4. Bio-sludge dewatering

After conditioning, the dewatering process was realized using a normalized filtration-expression cell (AFNOR 1979). The cell was a 270-mm-deep cylindrical stainless steel chamber with an internal diameter of 70 mm (Fig. 1). A perforated disk was located at the bottom of the cylinder in order to support the filter medium. Filter medium was polypropylene material with permeability of 8 L/dm<sup>2</sup>/min and a thickness of 0.70 mm. The flocculated bio-sludge was poured with the supernatant into the filtration cell. Then, the pressure on the piston was applied and controlled by pressurized air; it was fixed at 5 bars.

When filtration cell device is filled by the flocculated bio-sludge, a certain amount of the supernatant flows by gravity: this volume of water is called the

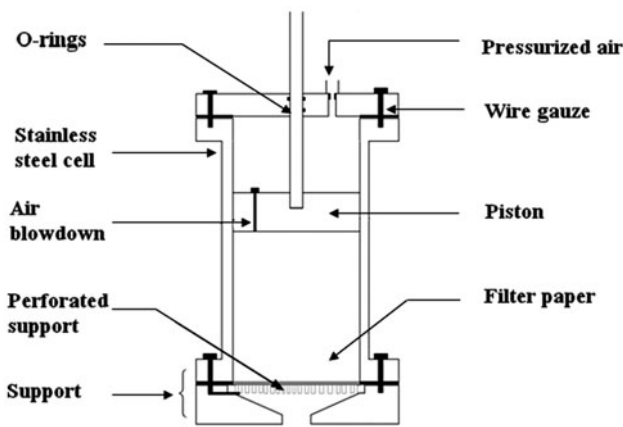


Fig. 1. Filtration-expression cell.

gravity drainage volume. This amount of water is in principle not taken into account to estimate the total volume of filtrate, because at this stage, no pressure is still applied to the bio-sludge sample (the gravity drainage volume will be subtracted from the total volume of filtrate at the end of the experiment). The mass of the collected filtrate was recorded every 10 s on the personal computer linked to a precision balance device. The filtration was stopped after a time fixed at 1 h for all experiments.

The data obtained during the dewatering process were plotted using time divided by filtrate volume ( $t/V$ ) as the ordinate and filtrate volume as the abscissa (Fig. 2). In theory, mechanical dewatering under a constant pressure drop can be divided into two successive steps: filtration and expression stages. The filtration phase is characterized by the linear part and it corresponds to cake formation due to the accumulation of the solid particles on the surface of a filter medium. The second part represents the

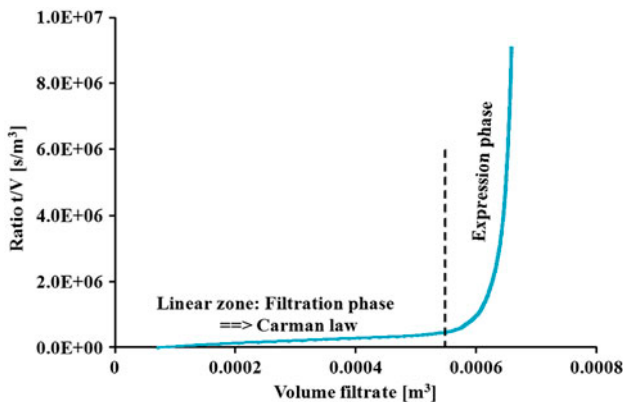


Fig. 2. Typical dewatering curve showing filtration and compression stages.

expression phase. It describes the removal of water by cake squeezing [15]. During the filtration phase, the ability of forming the cake to let the water go through is commonly characterized by the specific resistance to filtration (SRF) [15]. This parameter is classically calculated by the slope of the straight line portion of the graph according to Carman’s equation (Eq. (3)), based on Darcy’s law [16].

The end of the filtration phase can be obtained by linear fitting adjustment. To do so, the mean square error (MSE) (Eq. (4)) and the correlation coefficient  $R^2$  (Eq. (5)) were calculated; then, the fitted curve was determined using a defined program in Matlab software. A straight line was adjusted initially on the first five data points, and then the following points were added one by one. The end of the linear part corresponds to the experimental point from which MSE increases and  $R^2$  coefficient drops [17]. Fig. 3 shows the evolution of the two parameters (MSE and  $R^2$ ) as a function of the experimental points and the transition between the two area parts, indicated by the black line in the figure.

$$\frac{t}{V} = \mu \cdot \text{SRF} \frac{C}{2PA^2} V + \frac{\mu \cdot R_f}{PA} \tag{3}$$

$$\text{MSE} = \sqrt{\frac{\sum_{i=1}^n (y_i - x_i)^2}{n - q}} \tag{4}$$

$$R^2 = \frac{\sum_{i=1}^n (y_i - \bar{x})^2}{\sum_{i=1}^n (x_i - \bar{x})^2} \tag{5}$$

where  $x_i$  is the visualized values;  $\bar{x}_i$  is the mean of visualized values;  $\bar{y}_i$  is the fitting values,  $n$  is the number of observations,  $q$  is the modeling parameter number.

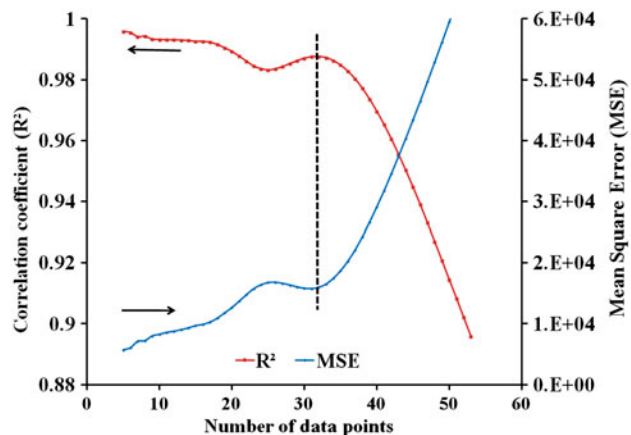


Fig. 3. Evolution of the two parameters ( $R^2$ , MSE) as a function of the considered experimental points for fitting Carman’s equation.

Before drying, bio-sludge cakes obtained after mechanical dewatering were extruded through a circular die of 14 mm of diameter and cut at a height of 14 mm, yielding cylindrical samples with a mass of approximately 2.5 g, as used in several industrial belt dryers.

### 2.5. Convective drying rig

Convective drying experiments (Fig. 4) were carried out in a so-called convective “micro-dryer,” specially designed for handling small extruded samples with a mass between 0.5 and 5 g. The micro-dryer is a classical convective rig controlled in relative humidity, temperature and air velocity, which has already been described in detail in a previous study [18].

Drying curves representing the drying rate ( $\text{kg}_{\text{dry air}}/\text{s}$ ) vs. the water content on a dry basis  $X$  ( $\text{kg}_{\text{water}}/\text{kg}_{\text{dry solids}}$ ) are obtained from these mass curves vs. time data. Dividing the drying rate by the external exchange area yields the so-called Krischer’s curves commonly used to study drying, i.e. the drying flux ( $\text{kg}_{\text{dry air}}/\text{m}^2 \text{s}$ ) vs. water content ( $\text{kg}_{\text{water}}/\text{kg}_{\text{dry solids}}$ ) depicted in Fig. 5. In accordance with the convective drying theory, three periods can be identified [19,20]:

- The first period, or the preheating period (AB), represents a period of adaptation of the sample to the drying conditions. During this period, the solid temperature and the drying rate increase considerably.

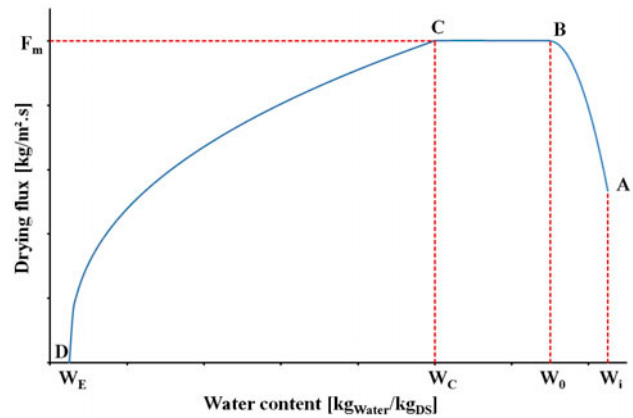


Fig. 5. Typical drying rate curve (Krischer’s curve).

- The second period (BC) is called the constant drying flux rate. During this period, the supplied heat serves essentially to the evaporation of the product water. As explained by Deng et al. [20], the evaporated water in this period is free water.
- The third period (CD) is the long-falling drying rate period, ending with stabilization in moisture content at an equilibrium value corresponding to the end of drying. In this period, the energy serves to evaporate the product water and to increase its temperature.

Results reported in this study refer to the following operating conditions: temperature of 130 °C, superficial velocity of 1 m/s, and the absolute humidity of the air fixed at 0.005  $\text{kg}_{\text{water}}/\text{kg}_{\text{dry air}}$ .

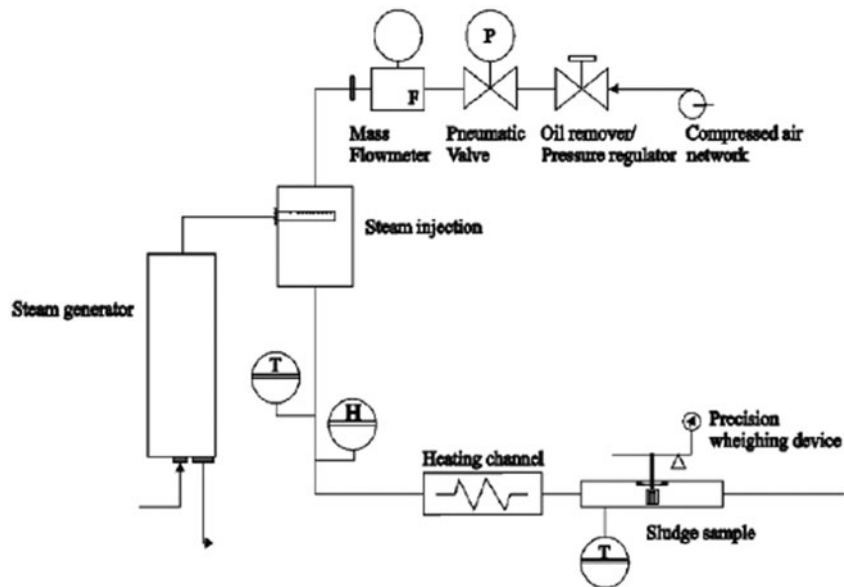


Fig. 4. Detailed scheme of the convective micro-dryer.

## 2.6. X-ray microtomography

To determine Krischer's curve, it is necessary to know the exchange surface developed by the bio-sludge sample, assumed to be the external sample surface. Following a method developed inside the laboratory [21,22], it was evaluated using X-ray microtomography, acting as a medical scanner. This method allows the determination of shrinkage curves from series of 2D cross section images of the sample. This results in a reduction in the effective surface exchange in the course of time. The X-ray microtomographic device used in this study was a "Skyscan-1074 X-ray scanner." The X-ray source operates at 40 kV and 1 mA. The detector is a 2D, 768 × 576-pixel, and 8-bit X-ray camera giving images with a pixel size of 41 μm. The following sequence was repeated several times during a drying experiment: drying interruption–tomographic analysis–drying resumption. These interruptions have been proved to not have impact on the drying kinetics [18].

## 2.7. Mathematical model and statistical analysis

An analysis of variances was used for graphical treatment of the data to obtain the evolution of the normalized sample volume  $V/V_0$  vs. the normalized water content  $X/X_0$ . Statistical tests were performed using Matlab software version 6.0; only shrinkage response was evaluated.

The goodness of fit of the model predictions to experimental values was evaluated under the condition of the root mean square error (RMSE) and the mean sum of square of errors (MSE) were used as criteria for accuracy of fitting. Then statistical significance was checked by dividing RMSE under MSE (RMSE/MSE); this variance ratio is called Fischer's  $F$ -test. Model terms were selected or rejected based on the  $F$  value that does not exceed a certain theoretical value ( $F^*$ ). This value was obtained using the desirability function  $\text{Finv}(1 - \alpha, v_1, v_2)$  available in Matlab software, where  $(1 - \alpha)$  is the confidence interval (CI) of the test,  $v_1$  and  $v_2$  are the number of degrees of freedom which represent the number of data points associated with, respectively, RMSE and MSE.

Some of these measures can be described as follows:

(a) Root mean square errors (RMSE)

It is signifying the noise in the data [23,24].

$$\text{RMSE} = S_e^2 = \frac{\sum_{i=1}^n \sum_{j=1}^{p_i} (Y_{ij} - \bar{Y}_i)^2}{(\sum_{i=1}^n p_i - n)} \quad (6)$$

(b) Mean sum of squares of errors (MSE)

It is defined like the mean square of the deviations between the experimental and calculated parameter levels [25].

$$\text{MSE} = S_r^2 = \frac{\sum_{i=1}^n (\bar{Y}_i - \hat{Y}_i)^2}{n - q} \quad (7)$$

where  $i$  represents to a particular selection of  $n$  independent variables;  $j$  is the number of replicates  $Y_{ij}$ ;  $p_i$  is the total number of replicates; the term  $(\sum_{i=1}^n p_i - n)$  is the number of degrees of freedom  $v$ ;  $\bar{Y}_i$  and  $\hat{Y}_i$  refer to experimental and calculated volume levels, respectively ( $Y = V/V_0$ );  $N$  represents the number of experimental data points and  $q$  stands for the number of constants used to calculate  $\hat{Y}_i$ .

(c) Fischer's equation ( $F$ -test)

$$F = \frac{\text{RMSE}}{\text{MSE}} \quad (8)$$

## 2.8. Experimental design

To evaluate the stability period of bio-sludge samples during storage, two types of experiments were performed. The experiments consist in performing the same conditioning, dewatering, and drying experiments on bio-sludge from the same WWTP but with different storage durations, in order to evaluate the effect of bio-sludge aging.

The Experiment "W" uses a sequence of one trial per beginning week. The first trial was done the day after the sampling to allow the bio-sludge sample to adapt to its new environment. This experiment was performed on three samples (a, b, and c) with one week apart, as shown in Table 1. This method allows comparing the variability of the sample for two successive weeks. Experiment "D" uses a sequence of one trial per day for one week, as illustrated on the same table. This experiment was performed on one sample (d). Because each trial needed a full day to completion, this constraint imposes that additional replicates were not performed on the same sample. Furthermore, the renewal of the sample for Experiment "W" provided more leanings.

In this article, the name of each sample is composed by one capital letter, one lowercase letter, and a number remembering, respectively, the name of the experiment, the name of the sample, and the number of storage days.

Table 1  
Experimental design for the two experiments

	Monday	Tuesday	Wednesday	Thursday	Friday
Week <i>i</i>	Sampling a	Wa1	–	–	–
Week <i>i</i> + 1	–	Wa8/ sampling b	Wb1	–	–
Week <i>i</i> + 2	–	Wa15	Wb8/ sampling c	Wc1	–
Week <i>i</i> + 3	–	–	Wb15	Wc8	–
Week <i>i</i> + 4	–	–	–	Wc15	–
Week <i>n</i>	Sampling d/ Dd0	Dd1	Dd2	Dd3	Dd4

Table 2  
Activated bio-sludge characteristics

Trials	Raw bio-sludge characteristics		Dewatering step <sup>a</sup>	
	Dry solids (%)	Volatile solids (%)	DS of dewatered cake (%)	SRF10 <sup>13</sup> (m/kg)
Wa1	1.04 ± 0.03	64.81 ± 0.49	16.67	3.16
Wa8	0.97 ± 0.01	62.47 ± 0.37	15.05	5.12
Wa15	0.88 ± 0.01	59.63 ± 0.52	14.17	6.13
Wb1	0.74 ± 0.01	64.56 ± 0.24	15.55	3.02
Wb8	0.68 ± 0.01	61.42 ± 0.75	14.19	4.92
Wb15	0.65 ± 0.02	58.71 ± 0.14	13.22	5.35
Wc1	0.78 ± 0.01	63.39 ± 0.43	17.44	3.35
Wc8	0.71 ± 0.65	60.65 ± 0.22	16.88	4.70
Wc15	0.65 ± 0.01	59.07 ± 0.65	14.92	7.17
Dd0	0.77 ± 0.01	66.30 ± 0.35	15.47	1.58
Dd1	0.77 ± 0.01	66.24 ± 0.03	14.68	1.35
Dd2	0.77 ± 0.01	66.19 ± 0.12	14.31	1.28
Dd3	0.76 ± 0.13	66.07 ± 0.72	14.69	1.07
Dd4	0.75 ± 0.01	66.19 ± 0.82	14.58	1.08

<sup>a</sup>Standard deviation cannot be established for the SRF and DS values; only one dewatering test was performed per day and provided a single dewatered cake, which extrudate samples will be tested in convective drying rig at the same day.

### 3. Results and discussion

In order to observe the influence of storage aging on activated bio-sludge, some bio-sludge parameters including DS and VS content of raw bio-sludge, SRF, DS values of dewatered cake are shown in Table 2.

#### 3.1. Impact of storage duration on the bio-sludge physical characteristics

In Experiment “W,” the DS data of raw bio-sludge decreased when the storage time increased and dropped to their lowest at 15 d after storage, displayed on column 2 of Table 2. The percentage of dry solids content loss between the first and fifteenth day is around 15% for all trials (see Wa, Wb, and Wc for details).

Looking at the first day of storage for Wa1, Wb1, and Wc1 samples, we can see that the sample of trial Wa1 is more concentrated than those obtained for Wb1 and Wc1. This could be explained by the fact

that bio-sludge samples were not collected at the same period of time. Indeed, human activity and meteorological terms may vary from one week to another, which is likely to influence the bio-sludge quality in terms of dry solids content. The analysis of VS values is also shown in this table in column 3. For all trials, it can be seen that the VS values decrease slightly after 8 and 15 d of storage from 63 to around 59%.

Concerning Experiment “D,” the DS values (Dd0, Dd1, Dd2, Dd3, and Dd4) are slightly stable from the first to the third day of the storage, with a light decrease in its values at the end of storage. About VS data, they were shown to be quite stable than those obtained in Experiment “W” but slightly higher.

Thus, storage in the case of Experiment “W” resulted in a reduction in the volatile solids content. This could be considered as an aerobic digestion process because of exposure to the continuous aeration and weathering effects during the long period of storage, up to 15 d. On the contrary, the VS values of

Experiment “D” remained almost constant. Based on these data, it can be concluded that a period of storage less than one week did not change significantly the characteristics of the raw material, indicating that no detectable aerobic digestion occurred during this short period of storage.

Usually, a bio-sludge containing less volatile solids content is easier to dewater [26], but it is not the only parameter which has to be taken into account. In fact, the dewaterability of activated bio-sludge can also be related to the particle size distributions of the flocs, EPS, and floc strength. According to Eriksson et al. [27], floc strength has been regarded as a key parameter, since flocs with poor strength easily deflocculate and thus decrease the dewaterability of the bio-sludge. A long period of storage is known to cause a deflocculation of the bio-sludge [28], but the key processes responsible for the change in floc strength are not well known. Finally, for this first approach, it is worthy to conclude that reducing storage time can have a beneficial impact on the next bio-sludge dewatering process, in terms of raw bio-sludge homogeneity.

### 3.2. Impact of storage duration on the dewatering process

The effect of storage duration on the dry solids content of dewatered bio-sludge is illustrated in column 4 of Table 2.

In the “W” series, the DS of the dewatered cake loses about 1% per week, implying that long bio-sludge storage has a negative impact on dry solids content of dewatered cake.

For the “D” series, performed on one trial per day, the DS values of the dewatered cake slightly decreased from 15.47 to 14.58% at the end of the experiment (Dd4). Nevertheless, an inexplicable value at the Dd2 sample was shown, maybe due to an experimental error. This result shows that reducing bio-sludge storage duration can avoid a decrease in dry solids content of bio-sludge after the dewatering stage.

In order to evaluate the sampling method on bio-sludge storage in terms of dewaterability, Fig. 6 presents the dewatering curves obtained for Experiment “W.” As discussed above, the dewatering kinetics of the different experiments could be divided in a fast filtration stage and a slow expression phase. The

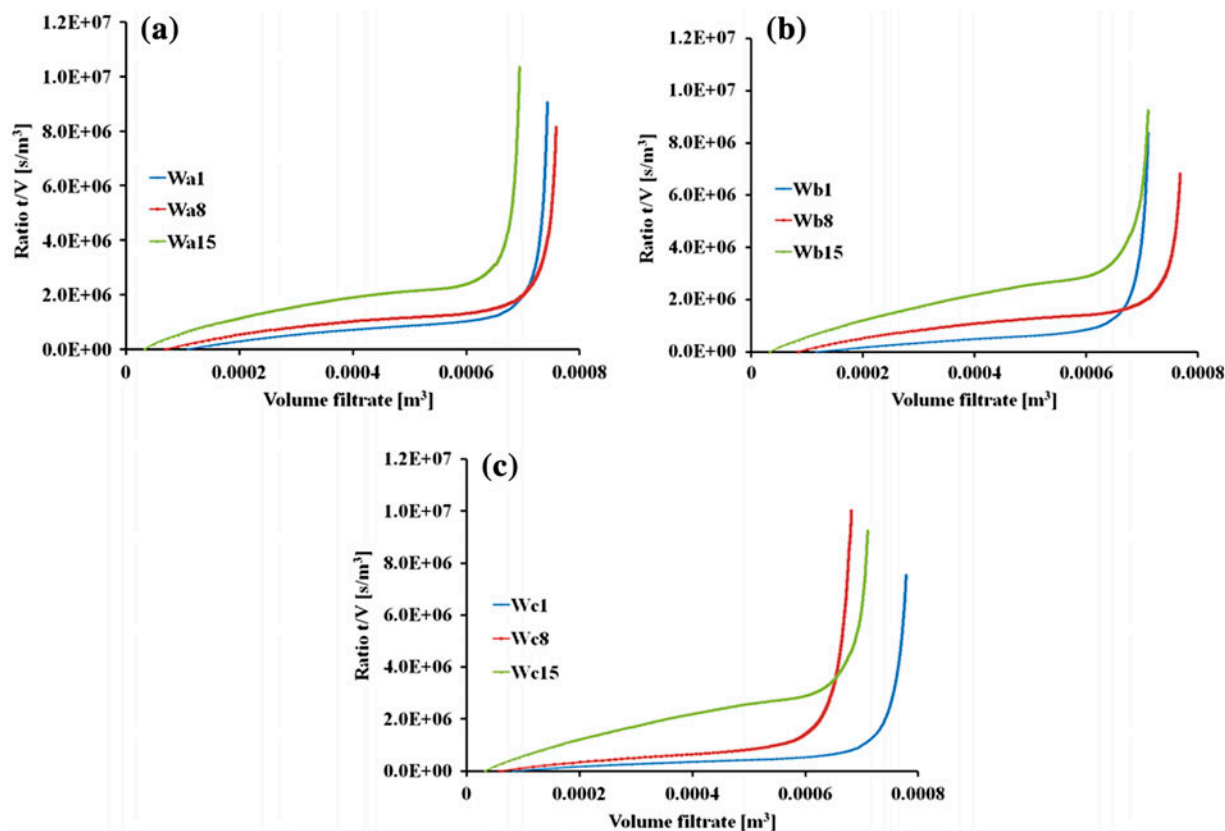


Fig. 6. Experiment “W” dewatering curves (a–c): were successively performed within 1 week of interval storage period.



dewatering behavior changed during storage as can be seen in that figure, mainly marked during the filtration stage with an increased value of the curve slope of the linear part from the first to the fifteenth day of storage. The general trend of curves of  $t/V$  vs.  $V$  results in a deviation from W1 to W15 curves. This deviation shows that the long storage of the bio-sludge (up to 15 d) changes the properties of the material: the phenomenon can be due to a bacterial degradation in which organic solids are decomposed into stable substances. Moreover, as we will see later, the SRF values calculated from the data provided by this figure (Table 2) tend to increase during storage, indicating a deterioration of the bio-sludge dewaterability.

Concerning Experiment “D” depicted in Fig. 7, dewatering behavior seems to be repeatable from the first to the last day of the test, with an increase in the kinetic expression phase at the end of the trials Dd0 and Dd4. However, it is noticed that there is also a slight shift at the beginning of these filtration curves, corresponding to the difference observed at the end of the expression phase. This difference can be explained by the fact that the initial volume of the filtrate after the correction of drainage gravity volume can vary, depending on the start time of applied pressure and the time step of computer data acquisition system. This leads to a value of initial filtrate volume which is two times higher for the tests Dd0 and Dd4 than it is for the other trials. This method finds its first limit, as the flocculated bio-sludge should be thickened by gravity drainage before its introduction into the filtration-expression cell device. Nevertheless, these dewatering curves all overlap (at the filtration stage) and

can be plotted along a master curve. This behavior (one master curve at filtration step) shows that the filtration stage does not seem to be affected by storage duration under a limited storage time. And then, the bio-sludge material can be well used to properly design an adequate experimental design.

After noticing that the bio-sludge daily behavior seems to be similar for the samples of Experiment “D,” it was interesting to know whether bio-sludge sampled at different periods of time could have similar behavior. Fig. 8 shows the different trials of all samples after one day of storage. As can be seen on the dewatering curves, the reproducibility seems to be reached at the filtration stage: all curves were almost overlapped. Consequently, bio-sludge samples can be stored for one working week. The following week, renewal of bio-sludge can produce a rather analogous behavior. Obviously, this assumption should always be verified.

After the dewatering tests, the SRF was calculated. The different values of this parameter according to the experimental trials are also given in the fourth column of Table 2. For Experiment “W,” the SRF values increased by a factor of two from the first to the fifteenth day of storage. It seems that storage duration reduces the yield of the dewatering process by increasing the SRF values. This result can be correlated with statements concerning the dry matter content of the dewatered cake: The more the DS values of the dewatered cake decrease with storage time, the poorer the bio-sludge filterability can be observed. The increase in SRF values can be attributed to the changes in the properties of the bio-sludge through chemical and microbiological processes during the long period

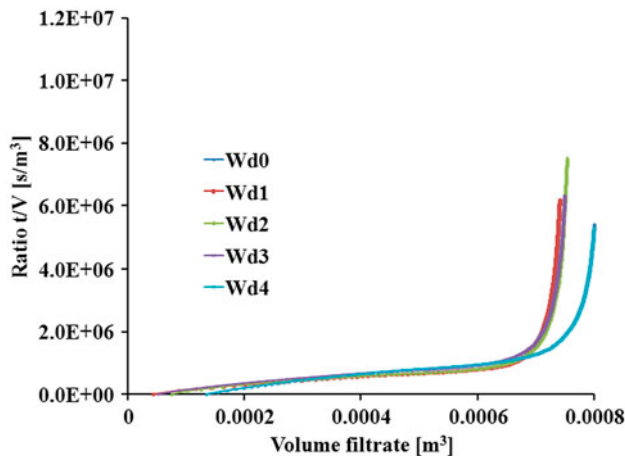


Fig. 7. Experiment “D” dewatering curves.

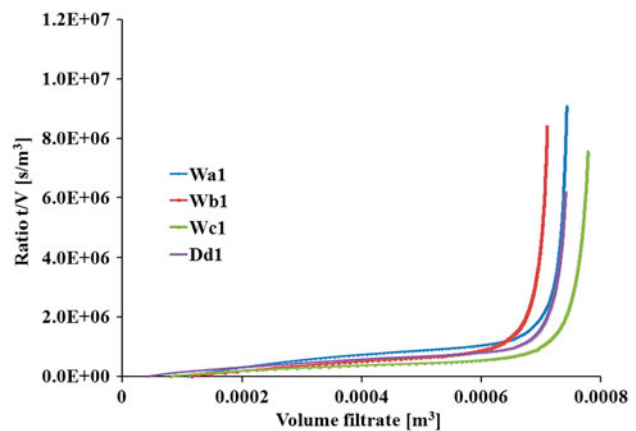


Fig. 8. Experiment “W” and “D” dewatering curves, at the first day of storage.

of storage. These changes strongly affect dewaterability, so the bio-sludge becomes much more difficult to dewater [28,29].

Concerning Experiment “D,” the deviation of SRF values is lower during bio-sludge storage even if a slow decrease was observed. Data were lower than those obtained for Experiment “W,” leading to a possible enhancement of bio-sludge dewaterability.

The high SRF values in the case of Experiment “W” can be explained by the changes in bio-sludge characteristics after a long period of storage as a result of bacterial degradation of organic matter and hydrolysis of exopolymers releasing colloidal particles [13]. These phenomena seemed to be responsible for reduced bio-sludge dewaterability.

Nevertheless, the importance of the use of SRF to express the ease of bio-sludge dewatering performance should be used with caution and remains controversial, as it can be difficult to achieve experimentally. Several reasons can be advanced: first, the so-called linear part of  $t/V$  vs.  $V$  (Carman’s law curve) is really not linear; as we can see in Fig. 6. Consequently, the SRF value might be difficult to assess accurately. Similar limitations concerning SRF evaluation using  $t/V$  vs.  $V$  dewatering curves were also observed by previous works [8,30]. Second, the detection of the filtration phase mainly depends on the number of points used to calculate the MSE as we have explained in the Materials and Methods section. These two reasons increase the difficulty to determine the exact numerical value of this parameter.

### 3.3. Impact of bio-sludge storage duration on the convective drying behavior

For convective drying experiments, two cylinder samples were cut, thanks to a pipe-shaped blade from the dewatered cake. Each sample was used to perform one specific experimental test: the first one was dried continuously to record mass loss, while the second one was removed several times from the dryer for tomographic investigation. Fig. 9 shows the mass loss of samples vs. time obtained, respectively, during drying at 1, 8, and 15 d of storage for the “W” series and drying curves at 0, 1, 2, 3, and 4 d of storage for the “D” series.

For the two series of experiments, classical drying curves are obtained showing the decrease in the mass of the sample plotted against the drying time. The images in Fig. 9 clearly show the impact of storage duration on the drying kinetics: For Experiment “W,” the change in mass loss vs. time shows significant discrepancies after a long period of storage (see

Fig. 9(a–c)), while within 5 d, the results can be considered as repeatable; all the curves were superimposed as can be seen in Fig. 9(d). It seems that, during the first 5 d, storage time does not affect the drying curve.

These results are partially in agreement with those obtained by Ferrasse et al. [12] studying another drying technique. These authors found that during indirect agitated drying of bio-sludge stored at 4°C, the results are different during the two first days after sampling and then remained the same until one week after sampling. It must be noticed that these tests were directly realized on bio-sludge dewatered within the wastewater treatment plant.

Convective drying results are usually expressed using Krischer’s curve, i.e. the drying flux vs. the water content [17]. Fig. 10 shows Krischer’s curves corresponding to the two series of experiments, based on surface evolution obtained using X-ray microtomography. As can be seen, regular patterns of drying rate curves are the same for the two types of experiments.

For the “W” series, poor repeatability is confirmed, with large differences during the falling drying flux period at 1, 8, and 15 d of storage (Fig. 10(a–c)). Accordingly, it can be emphasized that the old age of bio-sludge has, finally, a negative consequence on drying behavior. This phenomenon should be attributed to aerobic digestion processes occurring within a long storage time. On the contrary, good repeatability materialized by a single drying rate curve was obtained for the drying experiments after a weekly storage, as depicted in Fig. 10(d). This aspect should therefore be taken into account for establishing an appropriate experimental design.

Fig. 10 also indicates that, the maximum drying rate for sludge cake provided by Experiment “W” peaked around  $1.7 \times 10^{-3} \text{ kg/m}^2 \text{ s}$  globally for the three replicates of “W” (when the trial Wb15 was not considered), whereas the drying rate was found close to  $1.5 \times 10^{-3} \text{ kg/m}^2 \text{ s}$  for Experiment “D”. This comparison shows that the drying rate of “W” bio-sludge is slightly more important than the one observed for bio-sludge from Experiment “D”. This is not in agreement with Fraikin et al. [11] and Ferrasse et al. [12]. In their studies, these authors observed that the drying flux increased with reducing storage time, but their works were conducted on dewatered bio-sludge stored at 4°C, not on raw material.

Nevertheless, the difference observed above can be considered to be not significant and could be explained by the fact that the two samples were produced at an interval of 6 months, with possible changes in sludge quality. This highlights the difficulty in working with such a complex and versatile material.

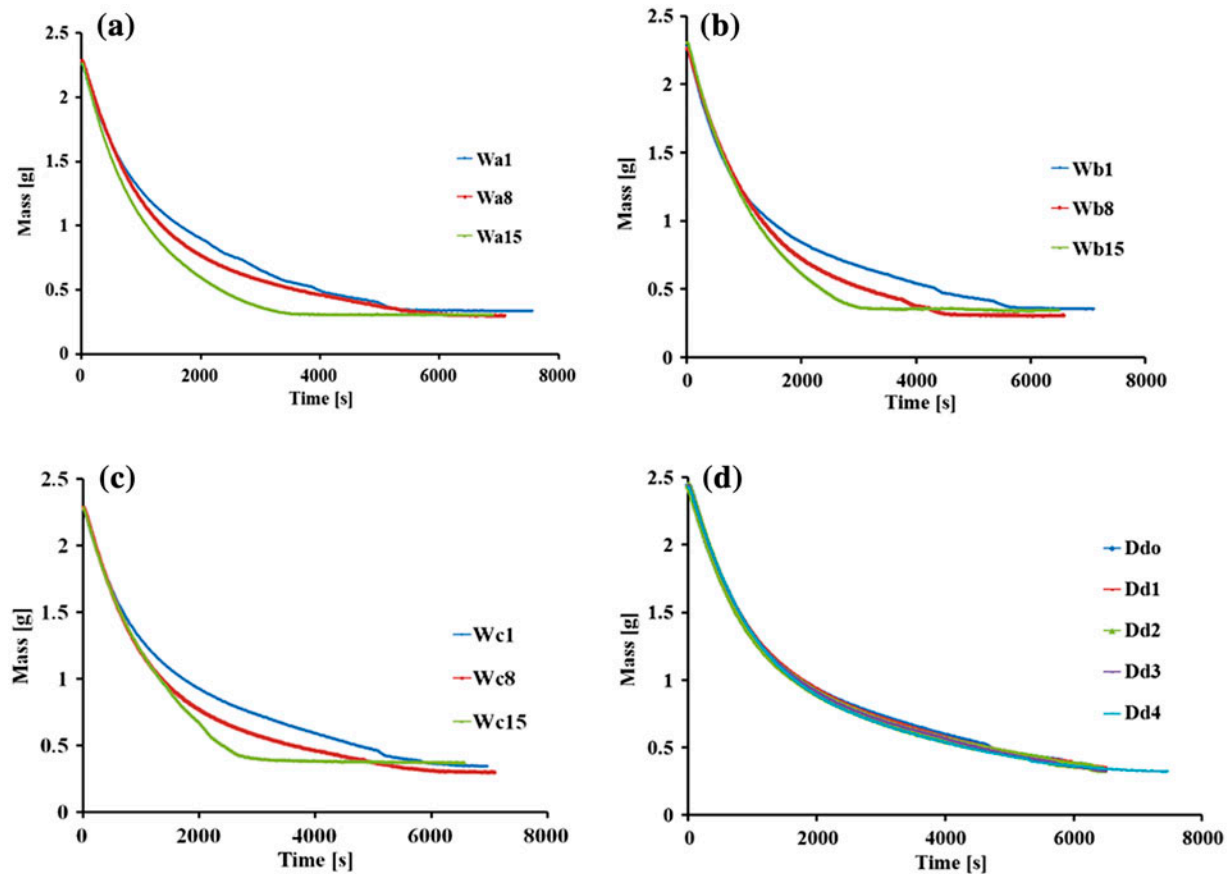


Fig. 9. Mass loss curves for the experimental design (a–c): Mass loss curves at 1, 8, and 15 d of storage ((b) and (c) as the replicates) (d): Mass loss curves at 1, 2, 3, 4, and 5 d of storage.

### 3.4. Shrinkage behavior during the drying process

During drying, the texture of the material evolves, including cracks/voids development. In order to get the drying flux and the final dimensions of the sampling bio-sludge after the end of drying experiments, intermittent drying experiments were done. To do so, the sample was temporarily removed of the micro-dryer every five minutes, for X-ray microtomography scanning for three minutes. Fig. 11 shows some scanning images of bio-sludge cake in the case of the Experiment “D” test after 5 d of storage. The first image located on the left side was a radiography of the initial wet sample, and the last right one was the corresponding image at the end of drying.

The wet cake sample is cylindrical in shape and uniform in interior density. When the sample was completely dry, volume shrinkage occurred simultaneously with crack development during drying.

These cross section images illustrate the decrease in the sample volume when its water content is progressively falling down. At approximately

$X = 2.350 \text{ kg}_{\text{water}}/\text{kg}_{\text{DS}}$ , the initial cracks that survived continued to develop in both width and length. No preferable orientation was noted for the cracks to be developed on the cake surface.

Comprehensive drying analysis should incorporate both volume shrinkage and a little bit of crack development, for better performance prediction of bio-sludge drying. Disregarding these parameters would inevitably incorrectly estimate the drying rate.

Fig. 12 shows the different shrinkage curves obtained and the corresponding fitting curves obtained using the X-ray microtomography method. These curves represent the evolution of the normalized sample volume  $V/V_0$  vs. the normalized water content  $X/X_0$ .

For all trials, the sample’s volume decreases linearly with decreasing moisture content until a  $X/X_0$  threshold value of around 0.3. Below this value, a break in slope materializing the beginning of the second period of shrinkage can be seen, indicated by the straight red line.

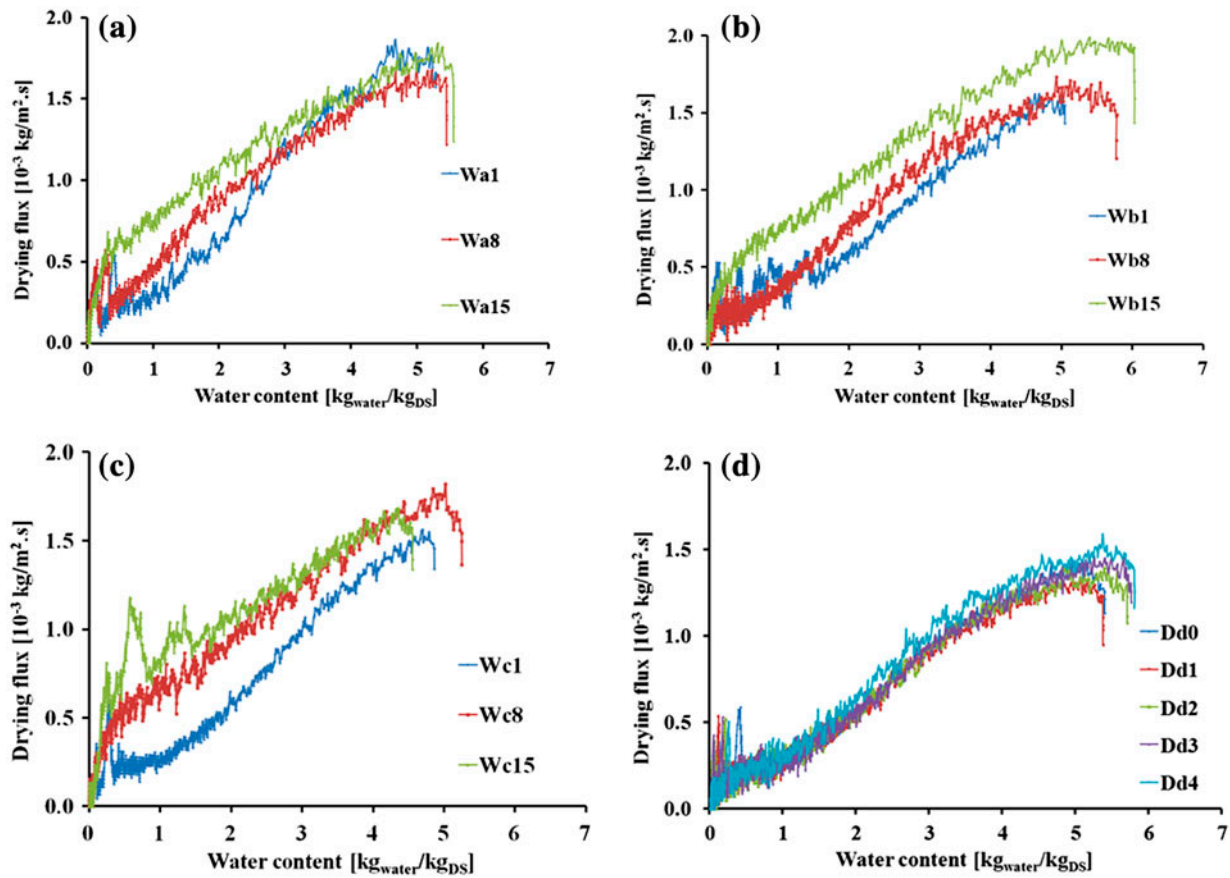


Fig. 10. Krischer's curves for the experimental design (a–c): Krischer's curves during drying at 1, 8, and 15 d of storage (b) and (c) as the replicates (d): Krischer's curves during drying at 1, 2, 3, 4, and 5 d of storage.

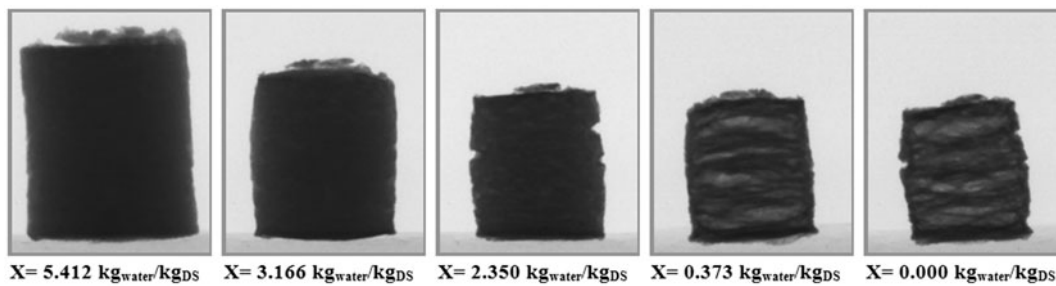


Fig. 11. Scanning images of crack development during drying (experiment "D").

According to this figure (Fig. 12), the first phase of the shrinkage curve is similar for all experiments. In the second phase, it seems that the storage time has an impact on the process, regarding the final volume of the bio-sludge that decreases progressively with increasing storage duration. Nevertheless, this phenomenon was not observed in the two cases Wa and Dd4, maybe due to an experimental error.

However, the results can be considered as repeatable, considering the number of trials showing a deviation of the second part of shrinkage curves to lower volumes during storage. This result is probably due to the evolution of intrinsic bio-sludge properties (such as viscosity, elasticity, etc.) during storage. Most probably, the "ideal" shrinkage stops earlier due to a change in the bio-sludge matrix mobility.

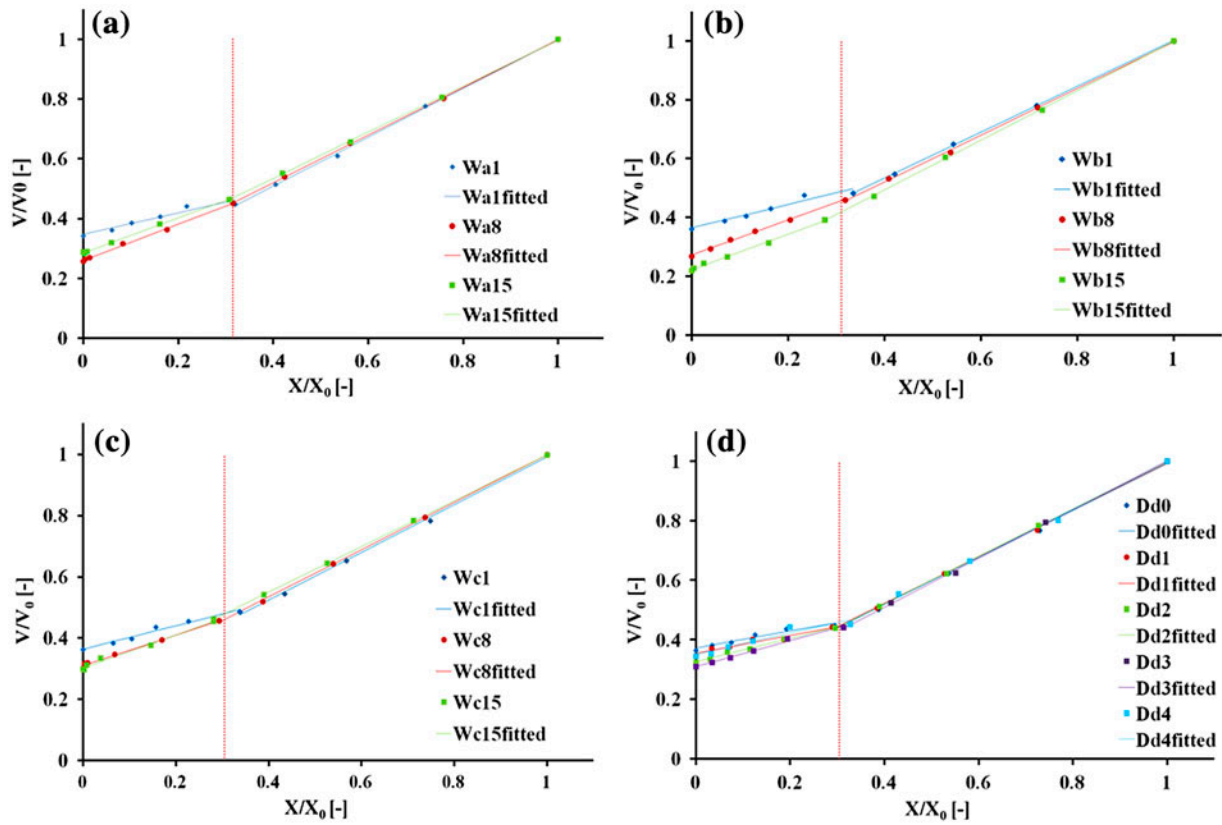


Fig. 12. Shrinkage volume vs. normalized moisture content (a–c): shrinkage volume for experiment “W” (d): shrinkage volume for experiment “D”.

To explain the observations mentioned above, it must be recalled that the bio-sludge sample contains two phases: solid and liquid water. During the first period, the volume shrinkage of the sample can be easily correlated with the quantity of evaporated water. The texture of the solid material does not hamper on the shrinkage process. During the second period, the structure of solid stiffens and then influences on the shrinkage phenomenon [31,32]. This phenomenon is essentially due to the properties of the material; water is replaced by air and porosity is created. Contrary to what was observed by Léonard et al. [32], during the second phase, a slowdown of shrinkage rather than definitive constant value appears.

To describe the shrinkage phenomenon that occurs during the drying process, linear models were selected. Thus, a first linear model based on the set of data points was tested. It has been rejected according to the bad shape of the shrinkage curves obtained. Inspired by the studies of Léonard et al. [32], a second model with two straight lines fitting was used. The mathematical modeling is given by the following forms:

$$\left. \begin{aligned} V/V_0 &= a_1 X/X_0 + b_1; & c < X/X_0 < 1 \\ V/V_0 &= a_2 X/X_0 + b_2; & X/X_0 < c \end{aligned} \right\} \quad (9)$$

where  $V/V_0$  and  $X/X_0$  are, respectively, the response and independent variables of the model,  $a_1$  and  $b_1$  represent the slope and ordinate parameters for the first part of the curve, and finally,  $a_2$  and  $b_2$  are the constants of the second part of the shrinkage curve equation. The value of  $c$  was identified by the method (Eq. (9)).

Table 3 shows the values of model coefficients and the corresponding statistical parameter  $F$ . The experimental value of the Fischer number was found to be inferior to the critical one  $F < F^*$  (IC = 95%;  $\nu_1 = 5$ ;  $\nu_2 = 50$ ;  $F^* = 2.4$ ). The model can be validated according to the method. Fig. 12 illustrates the adequacy between the calculated (called W or D/Fitted in the figure) and experimental values to describe shrinkage response in the experimental region investigated.

Table 4 displays the average water content and the volume of the sample at the break point  $((V/V_0)_{\text{threshold}}; (V/V_0)_{\text{threshold}})$  and also gives the final normalized volume obtained at the end of drying.

Table 3  
Fitting parameters of the shrinkage model

Fitting values	Wa1	Wa8	Wa15	Wb1	Wb8	Wb15	Wc1	Wc8	Wc15	Dd0	Dd1	Dd2	Dd3	Dd4
$a_1$	0.817	0.798	0.771	0.779	0.794	0.841	0.778	0.774	0.747	0.789	0.786	0.799	0.819	0.798
$b_1$	0.183	0.201	0.226	0.223	0.203	0.157	0.214	0.225	0.252	0.203	0.208	0.201	0.182	0.199
$a_2$	0.358	0.602	0.587	0.397	0.596	0.599	0.384	0.499	0.535	0.284	0.301	0.397	0.433	0.356
$b_2$	0.348	0.261	0.286	0.365	0.272	0.223	0.364	0.310	0.303	0.372	0.354	0.326	0.309	0.351
$F^a$	1.4	0.7	0.6	0.7	0.2	0.1	0.4	0.2	0.6	0.5	1.2	0.4	0.7	2.2

<sup>a</sup> $F$ : Corresponding statistical parameter of the model;  $a$  and  $b$  were, respectively, the slope and ordinate number of the linear model equation.

Table 4  
Break point characteristic and final shrinkage volume after drying

	$\overline{Wa}$			$\overline{Wb}$			$\overline{Wc}$			$\overline{Dd}$				
$(X/X_0)_{\text{threshold}}$	0.314			0.310			0.304			0.304				
$(V/V_0)_{\text{threshold}}$	0.455			0.445			0.466			0.444				
Days of storage	1	8	15	1	8	15	1	8	15	0	1	2	3	4
$(V/V_0)_{\text{final}}$	0.342	0.257	0.288	0.360	0.268	0.218	0.362	0.301	0.297	0.364	0.346	0.322	0.308	0.343

The values of break point coordinates were calculated by the average of the three trials of Experiment "W" and the five trials of Experiment "D".

The model (Eq. (9)) fitted on all experimental points is shown in Fig. 13. The first part of the curve (on the right) shows that the model can be considered good to describe shrinkage curves; all experimental points are almost superimposed. Under the break point, a slight dispersion of data points around the model was noticed, explained by the effect of storage duration. At this stage, it seems difficult to discriminate the two types of experiments, in terms of shrinkage behavior during storage.

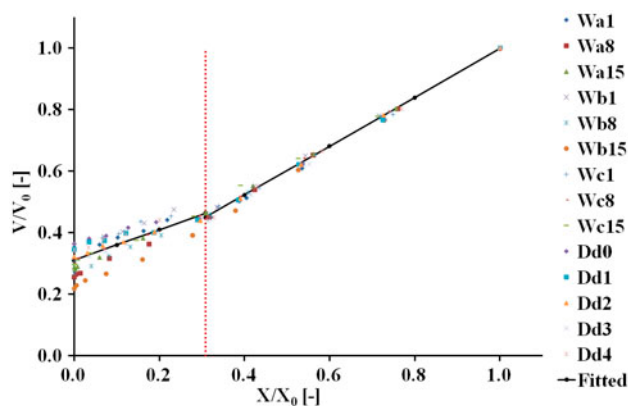


Fig. 13. Shrinkage volume vs. normalized moisture content for the experimental design.

#### 4. Conclusions

This first encouraging work was an attempt to put in evidence the impact of bio-sludge storage duration on both its dewatering and drying behaviors because bio-sludge is a complex living material in which its variability plays an important role. Two types of experiments were done: the first one for two successive weeks with a sequence of one trial at the beginning of each week (a, b and c) and the other for five working days with a sequence of one trial per day (see Table 1).

The dewatering process of the conditioned bio-sludge was experimentally studied using a normalized filtration-expression cell. Results indicated that from a storage time longer than a week, an increase in the SRF was observed, and, consequently, worse bio-sludge filterability was also observed.

Concerning convective drying, a good repeatability was observed for the drying curves obtained for five successive days from the collect day, whereas for bio-sludge stored for more than one week, different drying behaviors were obtained. In the case of the used polymer, it is advisable to use a bio-sludge sample for five days and to consider a weekly renewal.

During the drying process, shrinkage phenomenon was also observed in the bio-sludge samples. To characterize this shrinkage response, a linear model with two straight lines was developed. It was observed that the first part of the curve was almost

similar for all experiments, whereas the second part decreased progressively to lower volumes with increasing storage duration. This observation should be studied more to discriminate the two kinds of storage experiment behavior.

In future works, the impact of other polyelectrolytes' type and dosage at the laboratory scale, on the dewatering and drying processes will be investigated more deeply. Before each experimental design, the stability of the liquid bio-sludge will be evaluated using the approach presented in this work. Then, it should be recommended to evaluate the impact of storage duration on bio-sludge response prior to any study involving liquid bio-sludge.

### Acknowledgements

The authors thank Ciba Belgium Company for providing the Zetag 7587 flocculant. L. Fraikin is thankful to FRS-FNRS for its postdoctoral fellow positions (FRFC project 2.4596.12).

### Nomenclature

$A$	— filter section ( $\text{m}^2$ )
$C$	— ratio of mass of solid deposited by volume of the collected filtrate ( $\text{kg m}^{-3}$ )
CST	— capillary suction time (s)
DS	— dry solids content (%)
$i$	— particular selection of $n$ independent variables
$j$	— number of replicate $Y_{ij}$
$n$	— number of observations
$N$	— number of experimental data points and $q$ stands for the number of constants used to calculate $\hat{Y}_i$
Pa	— applied pressure (Pa)
$p_i$	— total number of replicates
$R_f$	— resistance of the filter medium ( $\text{m}^{-1}$ )
SRF	— specific resistance to filtration ( $\text{m kg}^{-1}$ )
$t$	— time (s)
$\mu$	— liquid viscosity (Pa s)
$V$	— volume of the filtrate ( $\text{m}^3$ )
$V_0$	— initial volume of the filtrate ( $\text{m}^3$ )
VS	— volatile solids content (%)
$W_d$	— total weight of the control including the weighting dish, after drying at $105^\circ\text{C}$ (g)
$W_p$	— tare weight of the weighting dish (g)
$W_q$	— total weight of the dried sample including the weighting dish, after calcination at $550^\circ\text{C}$ (g)
$W_r$	— tare weight of the weighting dish (g)
$W_s$	— weight of control, before drying (g)
$W_t$	— total weight of the dried residue obtained at $105^\circ\text{C}$ including the weighting dish (g)
WWTP	— wastewater treatment plant
$X$	— dry basis water content ( $\text{kg}_{\text{water}}/\text{kg}_{\text{DS}}$ )
$X_0$	— initial dry water content ( $\text{kg}_{\text{water}}/\text{kg}_{\text{DS}}$ )

$x_i$	— visualized values
$\bar{x}_i$	— mean of visualized values
$\bar{Y}_i$	— fitting values
$\bar{Y}_i, \hat{Y}_i$	— experimental and calculated volume levels, respectively

### References

- [1] C.d.l. Européenne, Directive 1991/271/EC du 21 mai relative au Traitement des Eaux Urbaines Résiduaires (European Board, Directive 1991/271/EC from 21 May, relative to Urban Residual Wastewater Treatment), 1991.
- [2] Infinity Communication, Traiter et Valoriser les Boues (recycling and treating sludge), Lavoisier TEC & DOC, Ligugé, 1997.
- [3] C.d.l.U. Européenne, Directive 1999/31/EC du 26 avril relative à la Mise en Décharge des Déchets (European Board, Directive 1999/31/EC from 26 April, relative to landfill of waste dump sites), 1999.
- [4] A.P.E. Sud-Aquitain, Surveillance Écologique des Sols par les Bioindicateurs, Aquitain (A.P.E. Sud-Aquitain, Ecological Monitoring Soil by Bioindicators, Aquitain), 2000.
- [5] C. Arthur Andersen, Examen de la Situation de la Filière de Recyclage Agricole des Boues d'Épuration Urbaines en Europe et dans divers autres Pays du Monde (Review of the State of Agricultural Recycling Filière of Urban Sludge Treatment of Europe and various other countries from Monde), Ademe ed., Environment Agency and Energy Management, Angers, 1999.
- [6] L.H. Mikkelsen, K. Keiding, Physico-chemical characteristics of full scale sewage sludges with implications to dewatering, *Water Res.* 36 (2002) 2451–2462.
- [7] C.F. Forster, Sludge surfaces and their relation to the rheology of sewage sludge suspensions, *J. Chem. Technol. Biotechnol.* 32 (1982) 799–807.
- [8] R. Konnur, S. Raha, J. Tanwar, S. Phanikanth, P. Pradip, P.C. Kapur, Data analysis and modeling of constant pressure batch dewatering of fine particle suspensions, *Dry. Technol.* 26 (2008) 1044–1059.
- [9] P. Arlabosse, J.H. Ferrasse, D. Lecomte, M. Crine, Y. Dumont, A. Léonard, Efficient sludge thermal processing: From drying to thermal valorisation, in: E. Tsotsas, A.S. Mujumdar (Ed.), *Modern Drying Technology*, vol. 4, Wiley-VCH Verlag GmbH & Co. KGaA, Hoboken, 2012, pp. 295–329 (Chapter 8).
- [10] M. Raynaud, J. Vaxelaire, P. Heritier, J.C. Baudez, Activated sludge dewatering in a filtration compression cell: Deviations in comparison to the classical theory, *Asia-Pac. J. Chem. Eng.* 5 (2010) 785–790.
- [11] L. Fraikin, T. Salmon, B. Herbreteau, J.-P. Levasseur, F. Nicol, M. Crine, A. Léonard, Impact of storage duration on the gaseous emissions during convective drying of urban residual sludges, *Chem. Eng. Technol.* 34 (2011) 1172–1176.
- [12] J.H. Ferrasse, P. Arlabosse, D. Lecomte, Heat, momentum, and mass transfer measurements in indirect agitated sludge dryer, *Dry. Technol.* 20 (2002) 749–769.
- [13] J.H. Bruus, J.R. Christensen, H. Rasmussen, Anaerobic storage of activated sludge: Effects on conditioning and dewatering performance, *Water Sci. Technol.* 28 (1993) 109–116.

- [14] A.D. Eaton, L.S. Clesceri, A.E. Greenberg, M.H. Franson, A.P.H. Association, Standard Methods for the Examination of Water and Wastewater, twenty first ed., APHA-AWWA-WEF, Washington, DC, 2005.
- [15] J. Vaxelaire, J. Olivier, Conditioning for municipal sludge dewatering. from filtration compression cell tests to belt press, *Dry. Technol.* 24 (2006) 1225–1233.
- [16] D. Mihoubi, J. Vaxelaire, F. Zagrouba, A. Bellagi, Mechanical dewatering of suspension, *Desalination* 158 (2003) 259–265.
- [17] A. Léonard, Étude du séchage convectif de boues de station d'épuration-Suivi de la texture par microtomographie à rayons X (Study convective drying of sewage-sludge Monitoring texture by X-ray microtomography), Faculté des Sciences Appliquées, Liège, 2003.
- [18] A. Leonard, S. Blacher, P. Marchot, M. Crine, Use of X-ray microtomography to follow the convective heat drying of wastewater sludges, *Dry. Technol.* 20 (2002) 1053–1069.
- [19] L. Bennamoun, M. Crine, A. Léonard, Convective drying of wastewater sludge: Introduction of shrinkage effect in mathematical modeling, *Dry. Technol.* 31 (2013) 643–654.
- [20] W. Deng, X. Li, J. Yan, F. Wang, Y. Chi, K. Cen, Moisture distribution in sludges based on different testing methods, *J. Environ. Sci.* 23 (2011) 875–880.
- [21] A. Léonard, S. Blacher, P. Marchot, J. P. Pirard, Measurement of shrinkage and cracks associated to convective drying of soft materials by X-ray microtomography, *Dry. Technol.* 22 (2004) 1695–1708.
- [22] A. Leonard, S. Blacher, P. Marchot, J.P. Pirard, M. Crine, Image analysis of X-ray microtomograms of soft materials during convective drying, *J. Microsc.* 212 (2003) 197–204.
- [23] V. Demir, T. Gunhan, A.K. Yagcioglu, A. Degirmencioglu, Mathematical modeling and the determination of some quality parameters of air-dried bay leaves, *Biosyst. Eng.* 88 (2004) 325–335.
- [24] Z. Wang, J. Sun, X. Liao, F. Chen, G. Zhao, J. Wu, Mathematical modeling on hot air drying of thin layer apple pomace, *Food Res. Int.* 40 (2007) 39–46.
- [25] A. Iguaz, M.B. San Martín, J.I. Maté, T. Fernández and P. Vírveda, Modelling effective moisture diffusivity of rough rice (*Lido cultivar*) at low drying temperatures, *J. Food Eng.* 59 (2003) 253–258.
- [26] J. Monod, *Mémento Technique de l'Eau*, Lavoisier, Rueil-Malmaison, 1989.
- [27] L. Eriksson, I. Steen, M. Tendaj, Evaluation of sludge properties at an activated sludge plant, *Water Sci. Technol.* 25 (1992) 251–265.
- [28] H. Rasmussen, J.H. Bruus, K. Keiding, Per Halkjær Nielsen, Observations on dewaterability and physical, chemical and microbiological changes in anaerobically stored activated sludge from a nutrient removal plant, *Water Res.* 28 (1994) 417–425.
- [29] J.T. Novak, G.L. Goodman, A. Pariroo, J.C. Huang, The blinding of sludges during filtration, *J. Water Pollut. Control Fed.* 60 (1988) 206–214.
- [30] M. Raynaud, J. Vaxelaire, P. Heritier, J.C. Baudez, Activated sludge dewatering in a filtration compression cell: Deviations in comparison to the classical theory, *Asia-Pac. J. Chem. Eng.* 5 (2010) 785–790.
- [31] J. Vaxelaire, J.R. Puiggali, Analysis of the drying of residual sludge: From the experiment to the simulation of a belt dryer, *Dry. Technol.* 20 (2002) 989–1008.
- [32] A. Léonard, S. Blacher, R. Pirard, P. Marchot, J.P. Pirard, M. Crine, Multiscale texture characterization of wastewater sludges dried in a convective rig, *Dry. Technol.* 21 (2003) 1507–1526.